1946 *Chem. Mater.* **2010,** *22,* 1946–1948
DOI:10.1021/cm9038768

CHEMISTRY OF MATERIALS
Communication

Solution-Based Growth of Monodisperse Cube-Like $BaTiO_3$ Colloidal Nanocrystals

Shiva Adireddy, Cuikun Lin, Baobao Cao, Weilie Zhou, and Gabriel Caruntu*

Advanced Materials Research Institute and the Chemistry Department, University of New Orleans, 2000 Lakeshore Drive, New Orleans, Louisiana 70148

Received December 30, 2009

There has been an increasing interest in the past few years in the synthesis of ferroelectric nanocrystals because of their scientific importance and widespread applications in electronics, sensing, catalysis, and nonlinear optics.[1] $BaTiO_3$ is a perovskite-type ceramic with unique mechanical, ferroelectric, electro-optic, pyroelectric, dielectric, and elastic properties that find use in multilayered capacitors, random access memories, thermistors, photonic crystals, pressure transducers, and waveguide modulators.[2] It is well-known that perovskite nanocrystals possess structural and physical properties that are strongly dependent on their size, shape, crystallinity, and surface composition. For example, in nanoscale $BaTiO_3$, the transition temperature from the ferroelectric (tetragonal) to the paraelectric (cubic) phase decreases progressively with the size of the particles as a result of a less distorted coordination environment of the Ti^{4+} ions within the TiO_6 octahedra. However, there is no clear consensus as to the critical size at which ferroelectricity is suppressed, and consequently, the values reported extend over a wide range, typically from 120 to 4.2 nm.[3] Despite the increasing number of solution-based methodologies proposed for the fabrication of nanoscale perovskites,[4] the synthesis of $BaTiO_3$ nanoparticles with controlled size and shape was met with limited success.[5] Nevertheless, free-standing, monodisperse $BaTiO_3$ nanocrystals with well-defined shape, controllable size and a high degree of compositional homogeneity are essential for the study of the ferroelectricity at nanoscale, as well as to open up new possibilities to assemble individual nanoparticles into functional nanostructures, such as 3D ferroelectric crystals and magnetoelectric multiferroic superlattices.

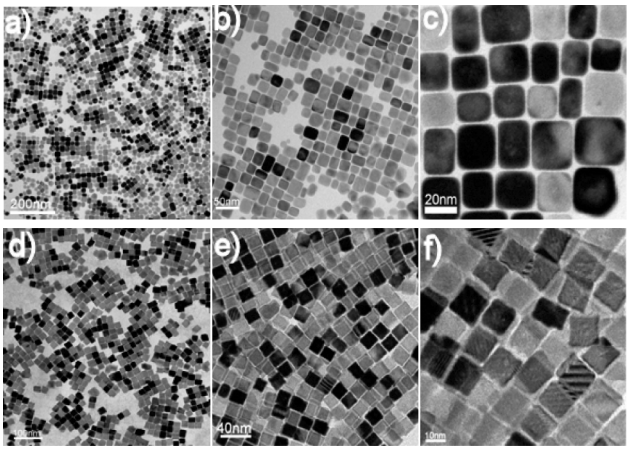

Figure 1. Bright-field TEM images of monolayers of (a−c) cubelike and (d) cubic $BaTiO_3$ nanoparticles. A bilayer of $BaTiO_3$ nanoparticles deposited on a microscope grid (e,f).

In this paper, we report on the controlled synthesis of free-standing, cubelike $BaTiO_3$ nanocrystals by a soft solution chemical process. The resulting nanocrystals retain oleic acid molecules on their surfaces and can be easily dispersed in nonpolar solvents. The experimental procedure was modified from that proposed by Li et al.[5b] and involves the thermal decomposition of metal fatty salts under hydrothermal conditions at temperatures as low as 135 °C. TEM and SEM images show that the $BaTiO_3$ nanoparticles are well-separated and have the tendency to self-organize into ordered domains on planar surfaces (Figures 1a−f). The atmosphere used during the preparation of the solutions before their transfer to the autoclave was found to influence the morphology of the $BaTiO_3$ nanocrystals. For example, when the solution was prepared in open atmosphere, only 36% of the nanocrystals were regular cubes (average edge length of 20 nm) whereas the main fraction (∼58%) was formed by cubelike nanoparticles with an aspect ratio varying from 1:1.05 to 1:1.81 (Figure 1a−c and the Supporting Information).

A small fraction of truncated cubes (∼6%) presumably resulting from an incomplete growth has also been detected. The nonunitary aspect ratio of the cubelike nanoparticles can be reasonably explained by the presence of $BaCO_3$

*Corresponding author.

(1) (a) Hennings, D.; Klee, M.; Waser, R. *Adv. Mater.* **1991**, *3*, 334. (b) Lines, M. E.; Glass, A. M. *Principles and Applications of Ferroelectrics and Related Materials*; Oxford University Press: Oxford, U.K., 2001. (c) Zhang, Z.; Sun, X.; Dresselhaus, M. S.; Ying, J. Y.; Heremans, J. *Phys. Rev. B* **2000**, *61*, 4850.
(2) (a) Bondurant, D.; Gnadinger, F. *IEEE Spectrum* **1989**, *26*, 30. (b) Li, X. *J. Mater. Sci.: Mater. Electron.* **2008**, *19*, 271. (c) Lott, J.; Xia, C.; Kosnovsky, L.; Weder, C.; Shan, J. *Adv. Mater.* **2009**, *20*, 3649. (d) Lee, H. G.; Kim, H. G. *J. Appl. Phys.* **1990**, *67*, 2024.
(3) (a) Park, Y.; Lee, W. J.; Kim, H. G. *J. Phys.: Condens. Matter* **1997**, *9*, 9445. (b) Spanier, J. E.; Kolpak, A. M.; Urban, J. J.; Grinberg, I.; Lian, O. Y.; Yun, W. S.; Rappe, A. M.; Park, H. *Nano Lett.* **2006**, *6*, 735. (c) Huang, T. C.; Wang, M. T.; Sheu, H. S.; Hsieh, W. F. *J. Phys.: Condens. Matter* **2007**, *19*, 476212.
(4) (a) Guangneng, F.; Lixia, H.; Xueguang, H. *J. Cryst. Growth* **2005**, *279*, 489. (b) Joshi, U. A.; Yoon, S.; Baik, S.; Lee, J. S. *J. Phys. Chem. B* **2006**, *110*, 12249. (c) Morerira, M. L.; Mambrini, G. P.; Volanti, D. P.; Leite, E. R.; Orlandi, M. O.; Pizani, P. S.; Mastelaro, V. R.; Paiva-Santos, C. O.; Longo, E. *Chem. Mater.* **2008**, *20*, 5381. (d) Huang, L.; Chen, Z.; Wilson, J. D.; Banerjee; Robinson, R. D.; Herman, I. P.; Laibowitz, R.; O'Brien, S. *J. Appl. Phys.* **2006**, *100*, 034316. (e) Bao, N.; Shen, L.; Srinivasan, G.; Yanagisawa, K.; Gupta, A. *J. Phys. Chem. C* **2008**, *112*, 8634. (f) Qin, S.; Liu, D.; Liu, H.; Zuo, Z. *J. Phys. Chem. C* **2008**, *112*, 17171. (g) Liu, H.; Hu, C.; Wang, Z. L. *Nano Lett.* **2006**, *6*, 1535. (h) Brutchey, R. L.; Morse, D. E *Angew. Chem., Int. Ed.* **2006**, *45*, 6564. (i) Niederberger, M.; Pinna, N.; Polleux, J.; Antonietti, M. *Angew. Chem., Int. Ed.* **2004**, *43*, 2270. (j) Huang, K. C.; Huang, T. C.; Hsieh, W. F. *Inorg. Chem. C* **2009**, *48*, 9180. (k) Demirors, A. F.; Imhof, A. *Chem. Mater.* **2009**, *21*, 3002.
(5) (a) O'Brien, S.; Brus, L.; Murray, C. B. *J. Am. Chem. Soc.* **2001**, *123*, 120. (b) Wang, X.; Zhuang, J.; Peng, Q.; Li, Y. *Nature* **2005**, *437*, 12.

 Published on Web 02/16/2010 © 2010 American Chemical Society

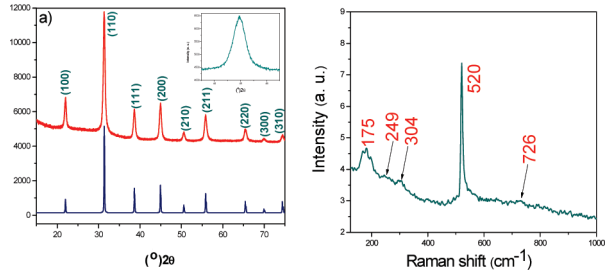

Figure 2. (a) X-ray diffraction pattern of the $BaTiO_3$ nanopowder. Bottom pattern represents the standard XRD pattern of cubic bulk $BaTiO_3$ (PDF 31−174).The inset represents a slow scan (step 0.002°, scan speed 0.00025°/s) of the (200) peak at room temperature; (b) Raman spectrum of the 22 nm cubelike $BaTiO_3$ nanoparticles.

detected in traces the XRD pattern of the sample. When the solution was prepared under an inert atmosphere the shape of the nanocrystals changed from cubelike to regular cubes with an average length edge of 22 nm (Figure 1d and Figure S3 in the Supporting Information). The size uniformity of the cubic nanocrystals allows them to assemble into ordered assemblies such as superlattices (Figure 1e,f). The XRD pattern of the cubic $BaTiO_3$ nanoparticles (Figure 2a) exhibits a series of well-defined peaks that can be indexed into a pseudocubic lattice, suggesting that the sample is single-phase and highly crystalline. Because it is well-known that the cubic and tetragonal polymorphs of nanoscale $BaTiO_3$ have a very similar crystal structure and in the absence of neutron diffraction data, the lattice parameter was indexed with the TREOR program[6] assuming a pseudocubic structure. The value obtained, a = 4.026(8) Å, is very close to those reported in the literature for both bulk tetragonal (d_{100} = 3.994 Å; d_{001} = 4.038 Å; JCPDS File No. 5−626) and cubic (d_{100} = 4.031 Å; JCPDS File No. 31−0174) $BaTiO_3$.[7] The average crystallite size calculated by the Scherrer formula[8] by fitting the line broadening of the three most intense peaks was found to be 21.3 nm which is consistent to the value obtained from TEM measurements indicating that the cubic nanoparticles are single crystalline. The HRTEM micrograph (Figure S2a, Supporting Information) shows well resolved lattice fringes along both diagonal directions of the nanoparticle. Each cubelike nanoparticle possesses {100} faceted edges and is free of defects such as stacking faults, dislocations, and grain boundaries. The calculated interplanar distance was 4.09 Å, which is consistent with the value reported for a pseudocubic perovskite structure.

On the basis of the shape of the nanoparticles and the type of terminal planes, we propose that the growth of the $BaTiO_3$ nanocrystals is accompanied by the development of low index facets such as the {100} planes, which significantly decrease the surface energy of the nanoparticles.[9] This assumption is consistent with theoretical modeling, which indicated that the {110} and {111} surfaces in $BaTiO_3$ crystals are less stable than the {100} faces because they are polar, and the large surface relaxation induces surface rumpling and instability.[10] The fast Fourier transform (FFT) of the HRTEM image shown in Figure S2b, (Supporting Information) further confirms the high crystallinity of the sample and the absence of lattice defects. The SAED image of the nanocubes (Figure S2c, Supporting Information) exhibits a series of concentric rings with a spotted appearance which can be ascribed to either cubic or the tetragonal $BaTiO_3$. Because the information provided by X-ray diffraction[11] is limited to the global structure of the crystal, we used vibrational spectroscopy experiments at room temperature to investigate the local distortions of the lattice. In Figure 2b is represented the Raman spectrum of the 22 nm cubic $BaTiO_3$ nanoparticles. Cubic $BaTiO_3$ (space group $Pm\bar{3}m$) is Raman inactive because of the isotropic distribution of the electrostatic forces (O_h symmetry) around the Ti^{4+} ions within each octahedron.[12] However, when the cubic symmetry is distorted, the resulting noncentrosymmetric tetragonal structure will lead to a splitting of the four, degenerate $3F_{1u}+F_{2u}$ modes into eight Raman active transverse (TO) and longitudinal (LO) phonons that are responsible for the anomalous Raman scattering.[13−15] Therefore, all the five distinct bands observed at 175, 249, 304, 520, and 726 cm^{-1} assigned to the A_1(LO), A_1(TO), B_1+E(TO+LO), E-(TO)+A_1(TO), and A_1(LO)+E(LO) modes in the Raman scattering profile of the as-prepared $BaTiO_3$ nanopowders clearly suggest the existence of an acentric structure due to a structural disorder of the Ti^{4+} ions within the TiO_6 octahedra.[16−18] No Raman bands corresponding to CO_3^{2-} ions (distinctive peaks at 1443 and 1730 cm^{-1}) were detected in the spectrum, confirming that the cubic $BaTiO_3$ nanoparticles obtained from solutions prepared under an inert atmosphere are free of $BaCO_3$. Steigewald and co-workers have ascribed the sharpness of the peak at 520 cm^{-1} to an increased structural coherence in the distorted TiO_6 octahedra, whereas its asymmetry is associated to the coupling of the transverse optical modes associated to the tetragonal structure.[19] Our experimental results strongly indicate the existence of tetragonal distortions in the cubelike $BaTiO_3$ nanoparticles although it is generally considered that such

(6) Kezler, D.; Ibers, J. A. *POLSQ: Program for Least-Squares Unit Cell Refinement*; modified by Cahen, D., Keszler, D.; Northwestern University: Evanston, IL, 1983.
(7) Waesche, R.; Denner, W.; Schulz, H. *Mater. Res. Bull.* **1981**, *16*, 497.
(8) West, A. R. *Solid State Chemistry and Its Applications*; John Wiley & Sons: London, 1984; p 174.
(9) Wang, Z. L. *J. Phys. Chem. B* **2000**, *104*, 1153.
(10) Xue, X. Y.; Wang, C. L.; Zhong, W. L. *Surf. Sci.* **2004**, *550*, 73.
(11) Du, H.; Wohlrab, S.; Weis, M.; Kaskel, S. *J. Mater. Chem.* **2007**, *17*, 4605.
(12) DiDomenico, M.; Wemple, S. H.; Porto, S. P. S. *Phys. Rev.* **1968**, *174*, 522.
(13) (a) Busca, G.; Ramis, G.; Gallardo Amores, J. M.; Sanchez Escribano, V.; Piaggio, P. *J. Chem. Soc., Faraday Trans.* **1994**, *90*, 3181. (b) Ikegami, S. *J. Phys. Soc. Jpn.* **1964**, *19*, 46. (c) Robins, L. H.; Kaiser, D. L.; Rotter, L. D.; Schenck, P. K.; Stauf, G. T.; Rytz, D. *J. Appl. Phys.* **1994**, *76*, 7487.
(14) Calos, N.; Forrester, J.; White, T. J.; Graves, P. R.; Myhra, S. *J. Mater. Sci.* **1995**, *30*, 4930.
(15) Dobal, P. S.; A. Dixit, A.; Katiyar, R. S.; Yu, Z.; Guo, R.; Bhalla, A. S. *J. Appl. Phys. B* **2001**, *89*, 8085.
(16) Asiaie, R.; Zhu, W.; Akbar, S. A.; Dutta, P. K. *Chem. Mater.* **1996**, *8*, 226.
(17) El Marssi, M.; Le Marrec, F.; Lukyanchuk, I. A.; Karkut, M. G. *J. Appl. Phys.* **2003**, *94*, 3307.
(18) Upendra, J. A.; Yoon, S.; Baik, S.; Lee, J. S. *J. Phys. Chem. B* **2006**, *110*, 12249.
(19) Smith, M. B.; Page, K.; Siegrist, T.; Redmond, P. L.; Walter, E. C.; Seshadri, R.; Brus, L. E.; Steigerwald, M. L. *J. Am. Chem. Soc.* **2008**, *130*, 6955.

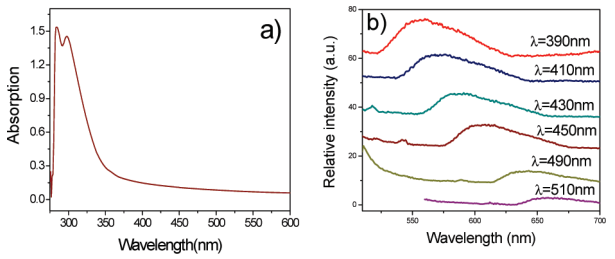

Figure 3. (a) UV−vis and (b) emission spectra of the cubelike $BaTiO_3$ nanoparticles.

distortions are local, that is, they involve several lattice constants and several vibrational periods, whereas the global structure of $BaTiO_3$ is still cubic.[19,20] Neutron diffraction experiments and piezoelectric force microscopy (PFM) studies are currently underway in order to elucidate the local structural distortions in the $BaTiO_3$ nanocubes. The UV−vis spectrum of the colloidal $BaTiO_3$ nanoparticles (Figure 3a) presents two peaks is observed at 284 and 298 nm, whereas the emission profiles present a broad characteristic peak covering a large part of the visible spectrum (Figure 3b).

This emission peak is red-shifted from 559 to 668 nm when the excitation wavelength is increased from 390 nm (2.43 eV) to 510 nm (3.18 nm), respectively. Because of its high symmetry, direct electron transitions from the valence to the conduction band are forbidden in bulk cubic $BaTiO_3$. Additionally, the pure material does not present intrinsic luminescence when the excitation energy is smaller than its band gap (E_g = 3.57 eV).[21] The band gap of the cubic $BaTiO_3$ nanoparticles calculated by fitting the linear portion of the curve of the variation of $(ah\nu)^{1/2}$ vs the photon energy led to a value of E_g = 3.2 eV, which is significantly smaller than that reported for the bulk material. Photoluminescence in nanostructured $BaTiO_3$ originates from the local distortion of the Ti^{4+} ions within the TiO_6 octahedrons, self-trapped excitons, oxygen vacancies, surface states or charge transfers via intrinsic defects inside an oxygen octahedron.[22−25] However, in our case, X-band electron paramagnetic resonance (EPR) spectroscopy studies did not reveal the existence of any oxygen or titanium defects associated to unpaired electrons which can potentially induce photoluminescence effects in the $BaTiO_3$ nanopowders. As such, we suggest that the photoluminescence in cubic $BaTiO_3$ nanoparticles results from electronic states localized in the band gap as a result of the off-center shift of the Ti^{4+} ions within the TiO_6 octahedra. This local distortion not only modifies the Ti−O bond lengths, but also induces noticeable changes in the dihedral angle thereby altering the interaction among the electronic distributions on the atoms of the cell.[26] The red shift of the emission bands can be ascribed to the formation of localized states with different energy levels, presumably linked to the specific atom arrangements.[27] As reported previously, the absorption of energy by a luminescent material does not necessarily result in emission of light. Electrons and holes in excited states may return to lower energy and ground states via radiative and/or nonradiative relaxations.[28] Deeper level defects are more prone to nonradiative recombination processes upon multiphoton relaxation inducing a non-Gaussian shape of spectra. Such an assumption also explains why emission bands for excitation wavelengths longer than 630 nm under excitation of 390 nm were not experimentally observed. Therefore, when the sample was excited by longer wavelengths, the photons can relax to energy levels via deeper defects, resulting in the red-shifted emissions experimentally observed (see Figure S7 in the Supporting Information).

In summary, high-quality, deagglomerated, and nearly monodisperse $BaTiO_3$ cubelike nanoparticles were synthesized by a modified solvothermal route at temperatures as low as 135 °C. The resulting colloidal solutions show excellent stability against aggregation allowing the colloidal $BaTiO_3$ nanocrystals to be used as building blocks for the design of ordered arrays or thin films for implementation into various functional devices. Raman spectroscopy data have indicated a local tetragonal of the nanopowders as a result of the existence of a Ti^{4+} disorder within the TiO_6 octahedra of the perovskite-type lattice. These results are supported by the photoluminescence properties, which confirmed that the off-center shift of the Ti^{4+} ions induce localized states in the band gap. A systematic study is under way to elucidate the formation mechanism, achieve size control and extend this methodology to other nanoscale ferroelectric perovskites. We expect that these findings will lead to a better understanding of the size effects and surface curvature on ferroelectricity at nanoscale and will open the door for the use of ferroelectric nanocrystals as building blocks in the design of complex hierarchical nanostructured composites.

Acknowledgment. This work was supported by the University of New Orleans through start-up funding and the Department of Defense through DARPA (Grant HR 0011-09-1-0047). We are indebted to Prof. Vijay John and Ms. Joy St. Dennis at Tulane University for help with Raman measurements and Dr. Daniela Caruntu for useful discussions and help with the TEM experiments.

Supporting Information Available: Experimental protocol and characterization of $BaTiO_3$ cube-ike nanoparticles (TEM images, EDX data, TGA/DSC profile, and FT-IR spectrum) (PDF). This material is available free of charge via the Internet at http://pubs.acs.org.

(20) (a) Shiratori, Y.; Pithan, C.; Dornseiffer, J.; Waser, R. *J. Raman Spectrosc.* **2007**, *38*, 1288. (b) Moreira, M. L.; Mambrini, G. P.; Volanti, D. P.; Leite, E. R.; Orlandi, M. O.; Pizani, P. S.; Mastelaro, V. R.; Paiva-Santos, C. O.; Longo, E.; Varela, J. A. *Chem. Mater.* **2008**, *2*, 5381. (c) M. P. Fontana, M. P.; Lambert, M. *Solid State Commun.* **1972**, *10*, 1.
(21) Ianculescu, A.; Gartner, M.; Despax, B.; Bley, V.; Lebey, T.; Gavrila, R.; Modreanu, M. *Appl. Surf. Sci.* **2006**, *253*, 344.
(22) Zhang, W. F.; Yin, Z.; Zhang, M. S. *Appl. Phys. A: Mater. Sci. Process.* **2000**, *70*, 93.
(23) Yu, J.; Sun, J. L.; Chu, J. H.; Tang, D. Y. *Appl. Phys. Lett.* **2000**, *77*, 2807.
(24) Lu, S. G.; Xu, Z. K.; Chen, H.; Mak, C. L.; Wong, K. H.; Li, K. F.; Cheah, K. W. *J. Appl. Phys.* **2006**, *99*, 064103.
(25) Yu, J.; Chu, J.; Zhang, M. *Appl. Phys. A: Mater. Science and Processing* **2002**, *74*(5), 645.
(26) Orhan, E.; Pontes, F. M.; Pinheiro, C. D.; Longo, E.; Pizani, P. S.; Varela, J. A.; Leite, E. R.; Boschi, T. M.; Beltran, A.; Andres, J. *J. Eur. Ceram. Soc.* **2005**, *25*, 2337.
(27) Orhan, E.; Varela, J. A.; Zenatti, A.; Gurgel, M. F. C.; Pontes, F. M.; Leite, E. R.; Longo, E.; Pizani, P. S.; Beltran, A.; Andres, J. *Phys. Rev. B* **2005**, *70*, 085113.
(28) Blass, G. Grabmaier, B. C. *Luminescent Materials and Applications*; Kitai, A., Ed.; John Wiley & Sons: New York, 2008.